Molecular Vision 2006; 12:1319-33 <http://www.molvis.org/molvis/v12/a149/>
Received 26 April 2006 | Accepted 6 October 2006 | Published 27 October 2006

Intraretinal lipid transport is dependent on high density lipoprotein-like particles and class B scavenger receptors

Nomingerel Tserentsoodol,[1] Natalyia V. Gordiyenko,[1] Iranzu Pascual,[1] Jung Wha Lee,[1] Steven J. Fliesler,[2] Ignacio R. Rodriguez[1]

[1]Laboratory of Retinal Cell and Molecular Biology, Section on Mechanisms of Retinal Diseases, National Eye Institute, NIH, Bethesda, MD, [2]Saint Louis University Eye Institute and Department of Pharmacological and Physiological Science, Saint Louis University School of Medicine, Saint Louis, MO

Purpose: In our companion paper we demonstrated that circulating lipoproteins enter the retina via the retinal pigment epithelium (RPE) and possibly Müller cells. In order to understand how these lipids are transported within the retina, expression and localization of the main proteins known to be involved in systemic lipid transport was determined.
Methods: Expression of ABCA1, apoA1 (the major HDL protein), SR-BI, SR-BII, CD36, lecithin:cholesterol acyltransferase (LCAT), and cholesteryl ester transfer protein (CETP) was determined by reverse transcriptase polymerase chain reaction (RT-PCR) and immunoblots. Localization was determined by immunohistochemistry using fresh monkey vibrotome sections and imaged by confocal microscopy.
Results: ABCA1 and apoA1 were localized to the ganglion cell layer, retinal pigment epithelium (RPE), and rod photoreceptor inner segments. ApoA1 was also observed associated with rod photoreceptor outer segments, presumably localized to the interphotoreceptor matrix (IPM). The scavenger receptors SR-BI and SR-BII localized mainly to the ganglion cell layer and photoreceptor outer segments; in the latter they appear to be associated with microtubules. LCAT and CETP localized mainly to the IPM.
Conclusions: The presence and specific localization of these well-known lipid transport proteins suggest that the retina employs an internal lipid transport mechanism that involves processing and maturation of HDL-like particles.

In our companion paper (Tserentsoodol et al.) [1] we used cholestatrienol (CTL), a fluorescent cholesterol analog [2], to image the uptake of circulating low density lipoprotein (LDL) by the rat retina. Circulating LDL is taken up by the RPE and, to a lesser extent, by Müller glial cells and is quickly delivered to different compartments within the retina, especially photoreceptor cells and their outer segments. Quantification of deuterated cholesterol uptake and turnover by mass spectroscopy following intravenous injection indicates that the rat retina may be capable of completely replacing its cholesterol every 6-7 days, assuming a linear process [1]. Considering the fact that normal serum cholesterol levels in humans are approximately 2 mg/ml (with approximately 1.4 mg/ml attributable to LDL) [3] and that animal cells require less than 300 μg/ml of LDL to survive, coupled with the apparent lack of LDL-receptor (LDLR) regulation in RPE cells [4,5], this replacement may be even more rapid in humans.

The mechanism of delivery of cholesterol and other lipids from the Müller cells and RPE to other areas of the retina is unknown. However, much is known about the proteins that perform this function in systemic lipid transport [6-8]. Using this knowledge we decided to examine the main proteins responsible for the systemic cholesterol efflux and transport in the retina.

The ABCA1 transporter [9-11] is responsible for the transport of apolipoprotein A1 (apoA1) [10-13], the major protein component of high-density lipoproteins (HDL), and apolipoprotein E (apoE) [14,15]. The expression and localization of apoE in the retina has been previously reported [16-20], being localized primarily to Müller cells and astrocytes, as well as RPE cells, but the expression and localization of apoA1 has not been reported. The other partners in the reverse cholesterol transport and efflux process are the class B scavenger receptors SR-BI, SR-BII, and CD36, and the enzymes lecithin-cholesterol acyltransferase (LCAT) and cholesteryl ester transfer protein (CETP) [21-23]. SR-BI and SR-BII are alternatively spliced isoforms of scavenger receptors responsible for HDL uptake by the liver [24,25]. The relationships between ABCA1, apoA1, SR-BI, and SR-BII in the reverse cholesterol pathway have been well studied [24-27]. The SR-BI receptor is an HDL receptor that mediates selective uptake of lipids from the HDL particle without the degradation of the HDL lipoproteins [24]. In the liver, these HDL-delivered lipids are eventually excreted by emulsification with bile acids [24,28]. CD36 has been well characterized in macrophages, where it is known to recognize oxidized phospholipid ligands in oxidized LDL [29] and is also known to facilitate the internalization of HDL [30]. Finally, LCAT [31] and CETP [32] are known to participate in the maturation of HDL particles and are critically important in systemic cholesterol efflux [33].

Correspondence to: Ignacio R. Rodriguez, National Eye Institute, NIH, Mechanisms of Retinal Diseases Section, LRCMB, 7 Memorial Drive, MSC0706, Bldg. 7 Rm. 302, Bethesda, MD 20892; Phone: (301) 496-1395; FAX: (301) 402-1883; email: rodriguezi@nei.nih.gov

In this study we demonstrate that the retina expresses many of the key proteins known to be involved in systemic lipid transport. The specific compartmentalization of these proteins within the retina suggests a novel mechanism of intraretinal lipid transport, which we describe herein.

METHODS

Rabbit anti-human apoA1, anti-human ABCA1, anti-human LCAT, anti-SR-BI, and anti-SR-BII antibodies were purchased from Abcam Inc. (Cambridge, MA). Rabbit anti-CD36 peptide polyclonal antibody was purchased from Cayman Chemical Inc. (Ann Arbor, MI). Rabbit anti-human CETP was purchased from BioVision Research products (Mountain View, CA). AlexaFluor® 488-conjugated isolectin GS-IB4 (*Griffonia simplicifolia* lectin) was purchased from Invitrogen Corp. (Carlsbad, CA). Unless otherwise indicated or specified, other reagents were used as purchased from Sigma/Aldrich (St. Louis, MO).

SDS-polyacrylamide gel electrophoresis (SDS-PAGE) and immunoblotting (western blot) analyses: Protein samples were mixed with NuPAGE® LDS sample buffer and NuPAGE® reducing agent (Invitrogen Corp., Carlsbad, CA) and incubated at 65 °C for 10 min. The samples (20 µg each) were separated in 4-12% NuPAGE® Novex Bis-Tris Gels running in 1x NuPAGE® MOPS SDS Running Buffer at room temperature for 50 min at 200V. The protein electrophoresis reagents and apparatuses were purchased from Invitrogen/NOVEX. The gels were transferred onto a PROTRAN®-nitrocellulose membrane (Schleicher and Schuell BioScience Inc., Keene, NH) using a Trans-Blot electrophoresis apparatus (Bio-Rad, Hercules, CA). The transfer was performed in NuPAGE® Transfer Buffer and 10% methanol at 30 V, 4 °C overnight. The membrane was equilibrated in 1x Tris-Buffered Saline pH 7.4 (TBS) Tween-20 for 15 min, and blocked in 1x TBS, pH 7.4, 5% Carnation nonfat milk and 1% Western Blocking Reagent (Roche Diagnostics Corp., Indianapolis, IN) for 2 h. Incubations with primary antibodies were performed overnight at 4 °C, followed by 1 h of incubation with anti-rabbit, anti-sheep (Pierce Biotechnology, Inc., Rockford, IL) and anti-mouse (Santa Cruz Biotechnologies, Inc., Santa Cruz, CA) IgG peroxidase conjugated secondary antibodies at a dilution of 1:50,000. Blots were developed on X-ray film using SuperSignal® West Pico Chemiluminescent Substrate (Pierce, Rockford, IL) after a 10-120 s exposure. The SeeBlue Plus2® Pre-Stained Standard (10 µl) and/or HiMark® prestained Standard (10 µl) were used for the estimation of molecular weights on the gels and blots (Invitrogen Corp.).

RT-PCR: Human retina total RNA was purchased from BD Biosciences (Mountain View, CA). cDNA was synthesized from 2 µg of total RNA in a 20 µl reaction, using SuperScript III® Reverse Transcriptase (Invitrogen). PCR was performed using 1µl of the RT reaction as template. The amplification were performed using Platinum blue PCR supermix (Invitrogen Corp, Carlsbad, CA) under standard conditions for 35 cycles. GAPDH was amplified for only 25 cycles. All of the PCR products were sequenced to verify authenticity. Multiple products were individually cloned and sequenced. The oligonucleotides used are listed in Table 1.

Immunohistochemistry of monkey retina: Vibrotome sections (100 µm) were prepared using a vibrating-blade microtome (Leica VT1000S, Microsystems Nussolch GmbH, Nussloch, Germany) equipped with a sapphire knife (Electron Microscopy Sciences, Hatfield, PA). The retina sections were blocked with 1X PBS containing normal goat serum (diluted 1:10, by vol.), 0.5% BSA, 0.2% Tween-20, and 0.05% sodium azide for 4 h at 4 °C. The monkey retina sections were incubated with primary antibodies overnight (see figure legends for dilutions). Cy5-conjugated donkey anti-mouse and Cy5-conjugated goat anti-rabbit secondary antibodies (Jackson ImmunoResearch Laboratories, Inc., West Grove, PA) were used at 1:1000 dilution for 4 h at room temperature. Alexa Fluor® 488-conjugated Isolectin GS-IB4 (1:500 dilution) was used to stain capillary endothelial cells (see above), while nuclei were counterstained with 4',6'-diamino-2-phenylindole (DAPI; 1 µg/mL in 1x PBS). The slides were mounted (GelMount®; Biomeda Corp., Foster City, CA) and kept in the dark until viewing.

RESULTS

Expression of well-known lipoproteins, transporters, and receptors in the retina: In order to determine if the components of a lipid transport pathway are present in the retina, monkey retinas as well as two different human RPE-derived cell lines (APRE19 and D407) were analyzed for the expression of several well-studied molecules involved in systemic lipid and reverse cholesterol transport [21,23,33]. The expression of protein was determined by immunoblot (Western) analysis using monkey retina extracts (Figure 1A). The corresponding mRNA expression was assessed by RT-PCR using human retina RNA (Figure 1B). Both methods detected expression of ABCA1, apoA1, apoE, the scavenger receptors SR-BI, SR-BII, and CD36, as well as LCAT, and CETP in the retina. Our detection of apoE, is in good agreement with prior reports [16-20], and is included here for the sake of completeness, to correlate with the detection and localization of related components involved in the lipid transport process. We also include the RT-PCR results for apoB and LDLR here, while the corresponding protein expression and localization results are reported in our companion paper [1]. RT-PCR for LCAT demonstrated 3 distinct product bands, each of which was individually cloned and sequenced. The smaller product (297 bp) is the correct form of LCAT. The middle-size product (377 bp) is an alternatively splice variant of LCAT, represented by GenBank ESTs with accession numbers AW603466, AW842184. The largest product (471 bp) seems to be a genomic fragment, since it contains introns 2 and 3 and was not represented by GenBank ESTs.

Since the retina is a complex tissue composed of at least ten different cell types, we employed correlative immunocytochemical analysis to determine the cellular localization of the above mentioned proteins, in order to gain insights into their function within the retina.

Localization of ABCA1 and apoA1: The lipids present in LDL and molecules such as CTL [1] are highly insoluble in aqueous media. Hence, there must be a transport mechanism by which these lipids can move from the initial areas of uptake (e.g., RPE, Müller cells) to other cells within the retina, especially the photoreceptors. The ATP-binding cassette (ABC) superfamily of proteins are potential candidates to mediate this process. Most members of this family are involved in lipid transport [9-11]. The ABCA1 transporter has been well-studied and is known to form a complex with apoA1 and transport the lipoprotein complex out of the cells as HDL particles [10,11,13]. Immunohistochemical localization of ABCA1 was performed on monkey retina vibrotome sections (see Material and Methods). The nuclei were counter-stained with DAPI (blue) and immunoreactivity to primary antibodies was detected using a Cy5-conjugated secondary antibody (red).

ABCA1 immunoreactivity was imaged in both the macula and peripheral areas of the monkey retina (Figure 2). ABCA1

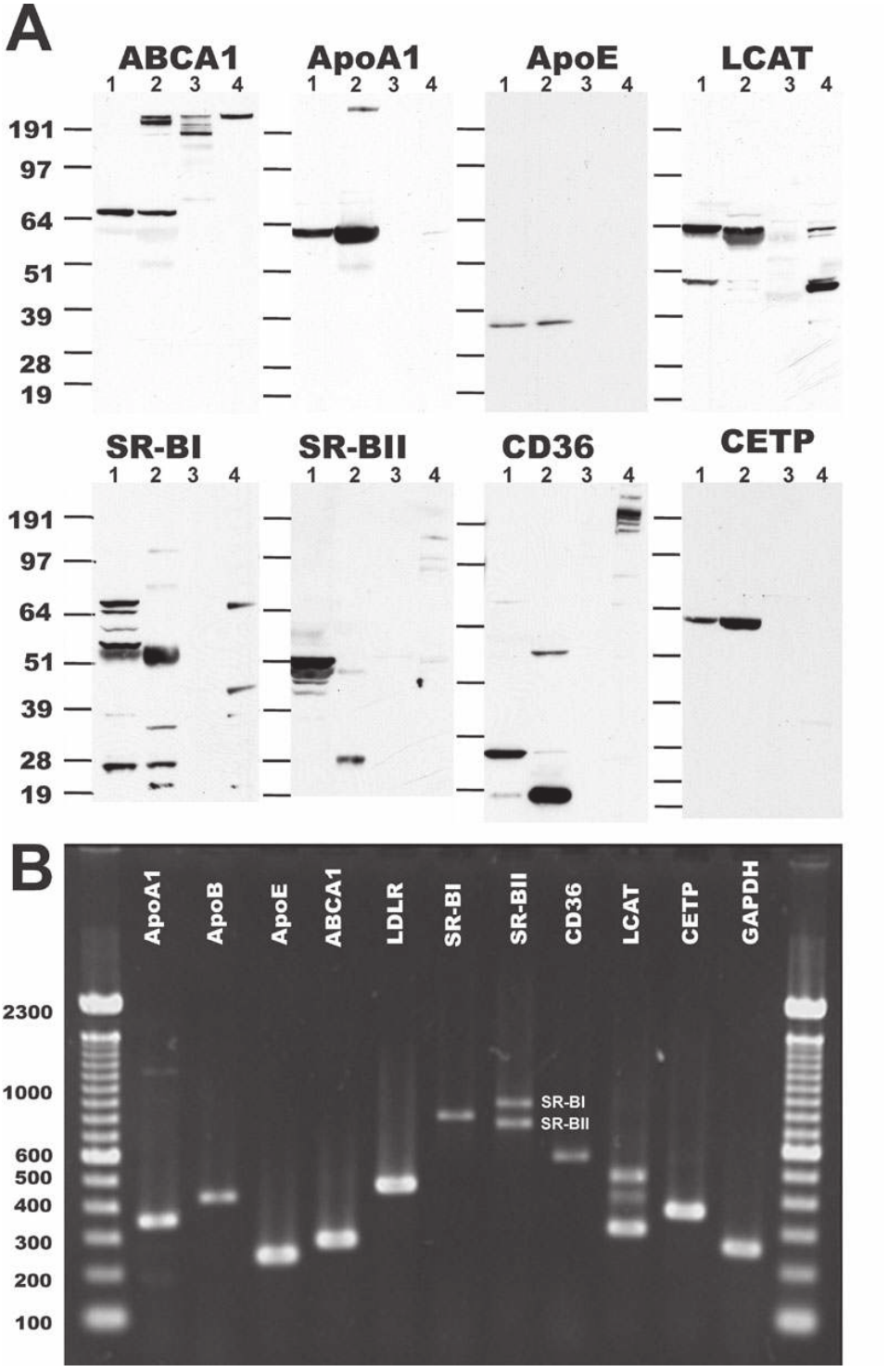

Figure 1. Expression of lipid transport proteins in human and monkey retina. **A**: Immunoblots of protein extracts from monkey retina and human RPE-derived cells lines. The lanes are as follows: 1. Monkey neural retina; 2. Monkey RPE-CH, 3; ARPE19 cells; 4. D407 cells. **B**: reverse transcriptase polymerase chain reaction of lipid transport proteins from human neural retina. The primers used and size of the products are shown in Table 1. The primers used to amplify SR-BII also amplify SR-BI.

localized mainly to the ganglion cell layer (GCL) and outer plexiform layer (OPL) in both the macular (Figure 2A) and peripheral retina regions (Figure 2D). The greater intensity of the ABCA1 immunoreactivity in the macular GCL and OPL may be due to the larger number of ganglion cells (approximately five times more) in the macula versus the peripheral retina. The macular RPE was more intensely labeled (Figure 2C) than the peripheral RPE (Figure 2D); however, the reasons for this difference are currently unknown and will require further investigation.

ApoA1, an HDL marker protein and the lipoprotein best known to be transported by ABCA1 [13], was detected in multiple locations throughout the retina (Figure 3). Immunoreactivity was observed in the GCL, outer plexiform layer (OPL), choriocapillaris (CH), the photoreceptor outer segments (POS) and the inner segment of the rods, but not the cones (Figure 3C). The immunoreactivity in the CH likely originates from the serum, where apoA1 is abundantly present. A higher magnification view of apoA1 immunoreactivity in the GCL is shown in Figure 3D (a negative control image, using no pri-

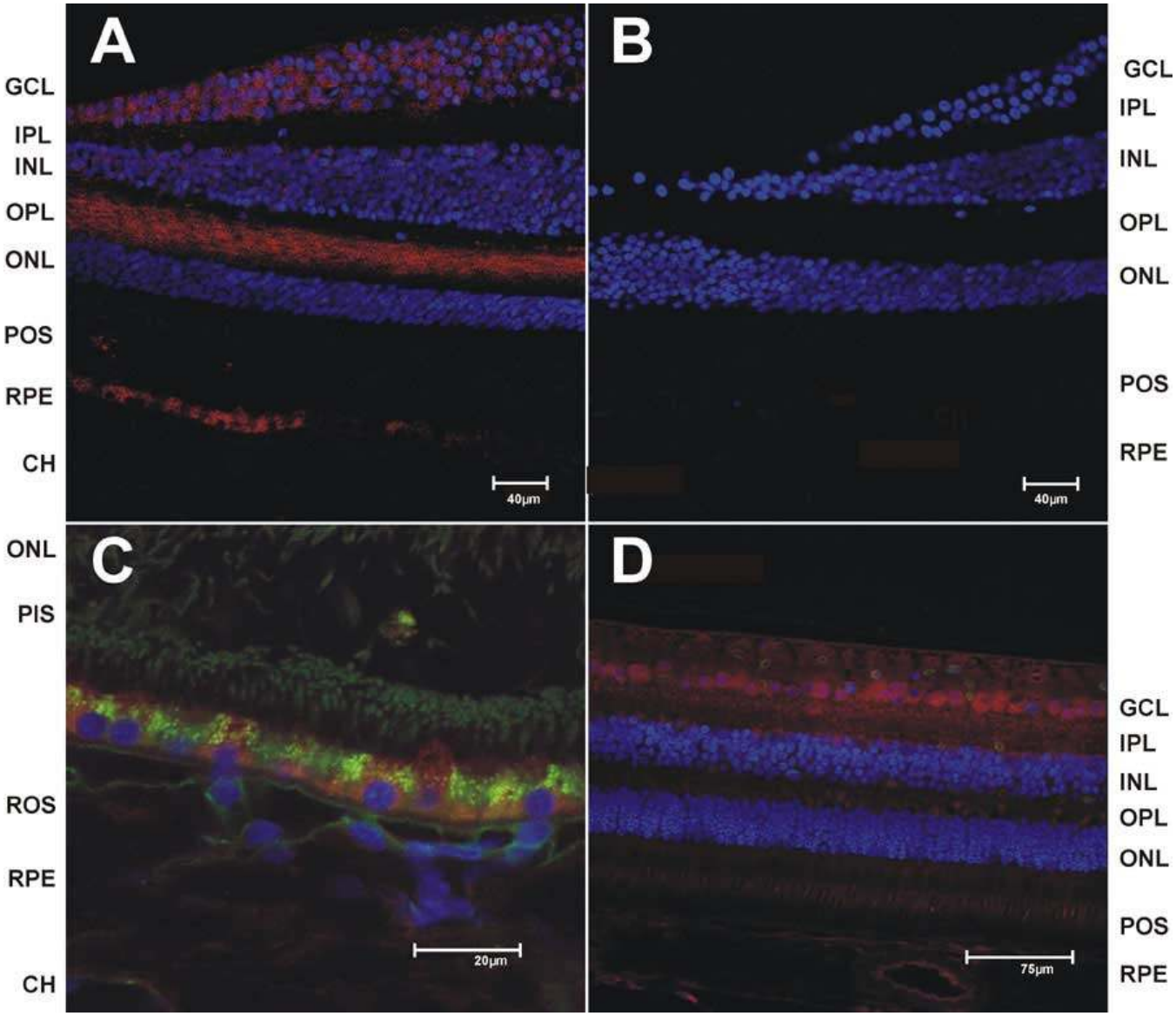

Figure 2. Immunohistochemical localization of ABCA1 in monkey retina. The vibrotome sections from monkey retina were processed for immunhistochemistry and imaged by fluorescent confocal microscopy (see Materials and Methods). Nuclei were stained with DAPI (blue) and immunoreactivity was detected using a Cy5 conjugated secondary antibodies (red). **A**: ABCA1 immunoreactivity in the macular (fovea) region of the retina was detected using anti-human ABCA1 rabbit polyclonal antibody (Abcam Inc.) at 1:500 dilution. **B**: No primary antibody control image of the macula. **C**: ABCA1 immunoreactivity at higher magnification focusing on the photoreceptors and macular retinal pigment epithelium. **D**: Low magnification image of the immunoreactivity in the peripheral retina. Images **C** and **D** are shown with the green channel to take advantage of the retinal autofluorescence and provide better structural definition. Capillaries in **D** were stained with isolectin IB4 (green). Scale bars were included with each image.

mary antibody, is shown in Figure 3B). Since apoA1 is a secreted, soluble lipoprotein, the POS-associated immunoreactivity is most likely due to localization of apoA1 within the interphotoreceptor matrix (IPM; Figure 3C). Bruch's membrane (usually not clearly visible under the conditions employed) was robustly labeled, definitively demonstrating the presence apoA1 in this extracellular interface between the RPE and the CH (Figure 3C). Notably, the RPE was labeled in the apical, but not the basal, aspect (Figure 3C), suggesting possible secretion of apoA1 by the RPE into the IPM.

Localization of class B scavenger receptors SR-BI, and SR-BII, and CD36 in monkey retina: The SR-BI receptor and it's alternatively splice variant, SR-BII, have been previously reported to localize to the RPE [34,35]. However, a complete description of the localization of these receptors in other compartments of the retina has not been reported heretofore. Using antibodies specific to each isoform, SR-BI and SR-BII were localized in the monkey retina.

In the neural retina, SR-BI immunoreactivity was localized to the ganglion cell layer (GCL) and possibly Müller cells,

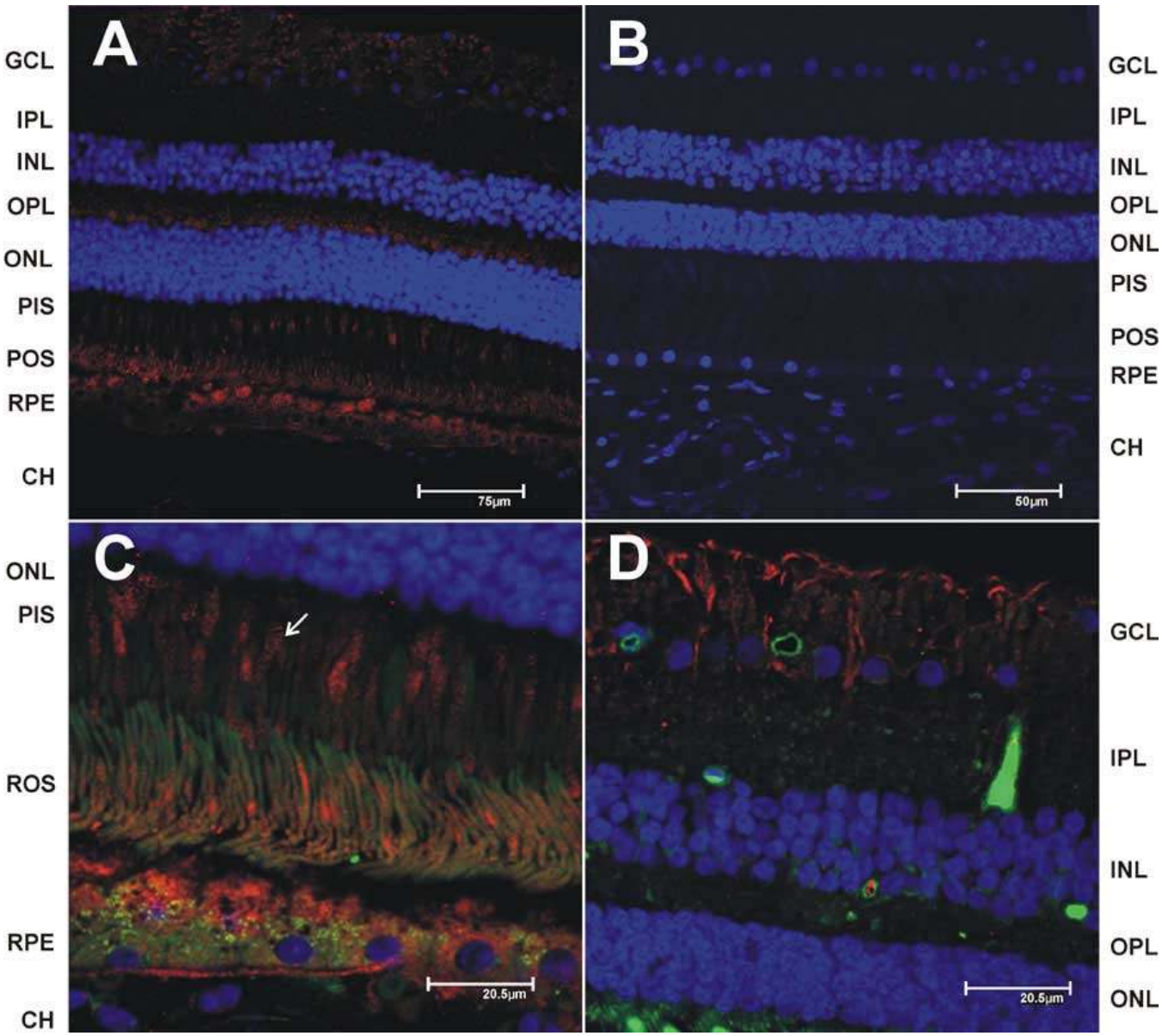

Figure 3. Immunohistochemical localization of apoA1 in monkey retina. The vibrotome sections from monkey retina were processed for immunhistochemistry and imaged by fluorescent confocal microscopy (see Materials and Methods). Nuclei were stained with DAPI (blue) and immunoreactivity was detected using a Cy5 conjugated secondary antibodies (red). **A**: ApoA1 immunoreactivity detected with anti-human apoA1 rabbit polyclonal antibody (Abcam Inc.) at 1:50 dilution. **B**: Control with no primary antibody. **C**: ApoA1 immunoreactivity at higher magnification focusing on the photoreceptors and retinal pigment epithelium/choriocapillaris regions, arrow points to the inner segments of the rod photoreceptors. **D**: Higher magnification of the ganglion cell layer. Images **C** and **D** are shown with the green channel to take advantage of the retinal autofluorescence and provide better structural definition. Capillaries in **D** were stained with isolectin IB4 (green). Scale bars were included with each image.

as well as to the photoreceptor outer segments and the choriocapillaris (Figure 4). SR-BI exhibited strong immunoreactivity particularly in the cone outer segments (Figure 4C) and the GCL (Figure 4D) although little or no immunoreactivity was observed in the RPE (Figure 4C).

SR-BII localized to similar regions as SR-BI (Figure 5), except the RPE was more heavily labeled, especially in the apical aspect (Figure 5C). Both receptors, particularly SR-BII, had a decidedly asymmetric, polarized distribution within the photoreceptor outer segments, preferentially labeling the side proximal to the connecting cilium and extending longitudinally along most of the outer segment length (Figure 5D). This asymmetrical pattern is even more apparent in cross sections of the retinal outer segments at or near the level of the connecting cilium (Figure 5D), both in rods (the smaller diameter profiles) and cones (the larger diameter profiles). This spatial

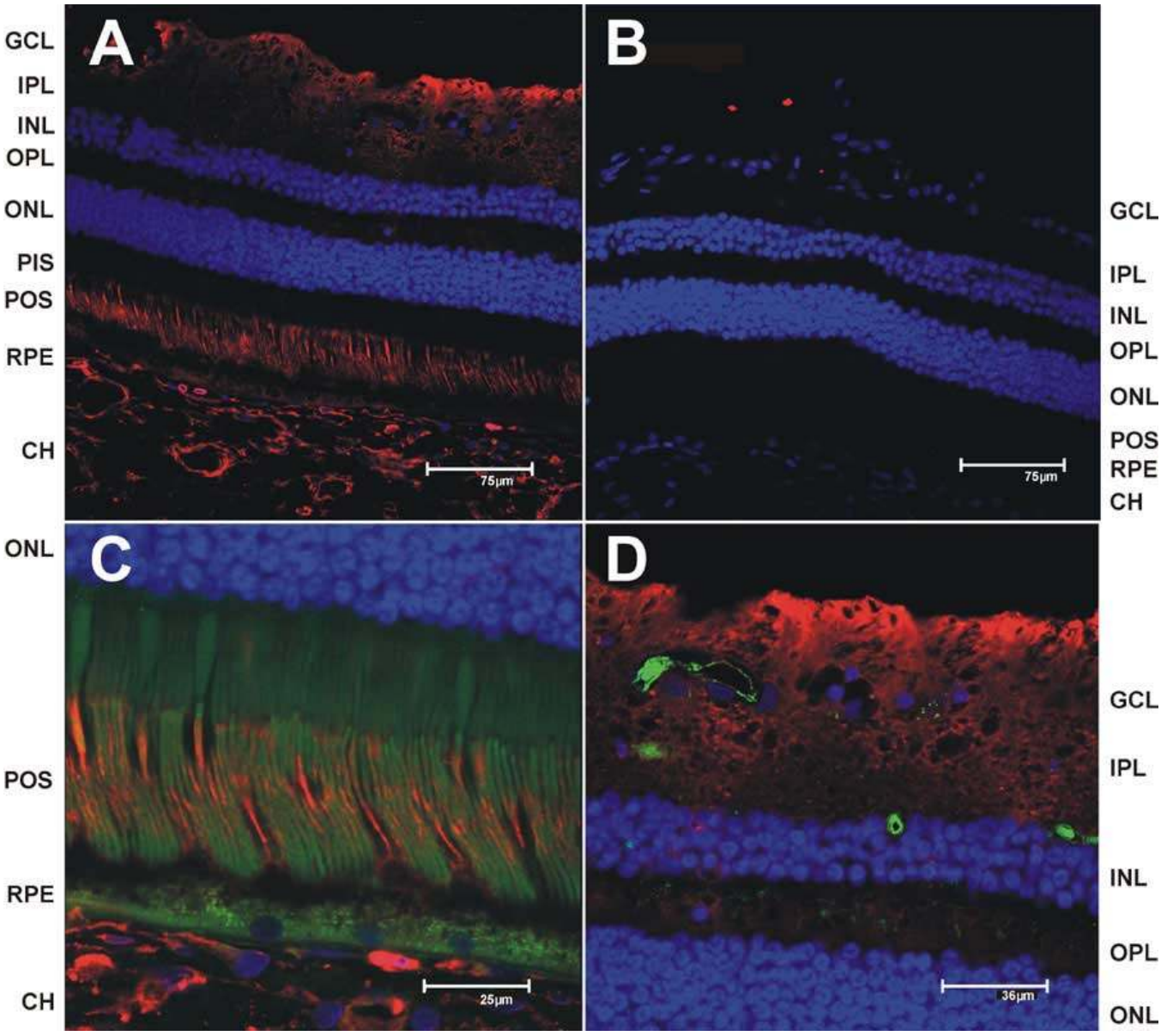

Figure 4. Immunohistochemical localization of SR-BI in monkey retina. The vibrotome sections from monkey retina were processed for immunhistochemistry and imaged by fluorescent confocal microscopy (see Materials and Methods). Nuclei were stained with DAPI (blue) and immunoreactivity was detected using a Cy5 conjugated secondary antibodies (red). **A**: SR-BI immunoreactivity detected using anti SR-BI peptide SPAAKGTVLQEAKL (cross-reacts with many species) rabbit polyclonal antibody (Abcam Inc.) at 1:100 dilution. **B**: No primary antibody control. **C**: SR-BI immunoreactivity at higher magnification focusing on the photoreceptors and retinal pigment epithelium/choriocapillaris regions. **D**: SR-BI immunoreactivity at higher magnification focusing on the GCL regions. Images **C** and **D** are shown with the green channel to take advantage of the retinal autofluorescence and provide better structural definition. Images **C** and **D** are shown with the green channel to take advantage of the retinal autofluorescence and provide better structural definition. Capillaries were in **D** were stained with isolectin IB4 (green). Scale bars were included with each image.

distribution is consistent with an association with microtubules, which reside in this cellular compartment; however, this remains to be confirmed. A negative control image (leaving out the primary antibody) is shown in Figure 5B.

CD36, another Class B scavenger receptor known to mediate HDL uptake [36], was also localized in the monkey retina (Figure 6). CD36 immunoreactivity was localized to the GCL, OPL, PIS, RPE, and CH (Figure 6A). Particularly interesting was the labeling of the rod, but not cone, inner segments (Figure 6C). Ganglion cells and Müller cells were robustly labeled as were the photoreceptor synaptic terminals in the OPL (Figure 6D). In addition, the rod outer segment tips were brightly labeled, which is consistent with the known phagocytic function of CD36 in the RPE (Figure 6C) [37-40].

Expression of LCAT (lethicin-cholesterol acyltransferase) and CETP (cholesterol-ester transfer protein): LCAT and CEPT are well-studied proteins that are secreted by the liver into the blood and work in conjunction with ABCA1, apoA and the SR-B scavenger receptors to facilitate reverse cholesterol transport [21]. The expression of LCAT and CETP (Fig-

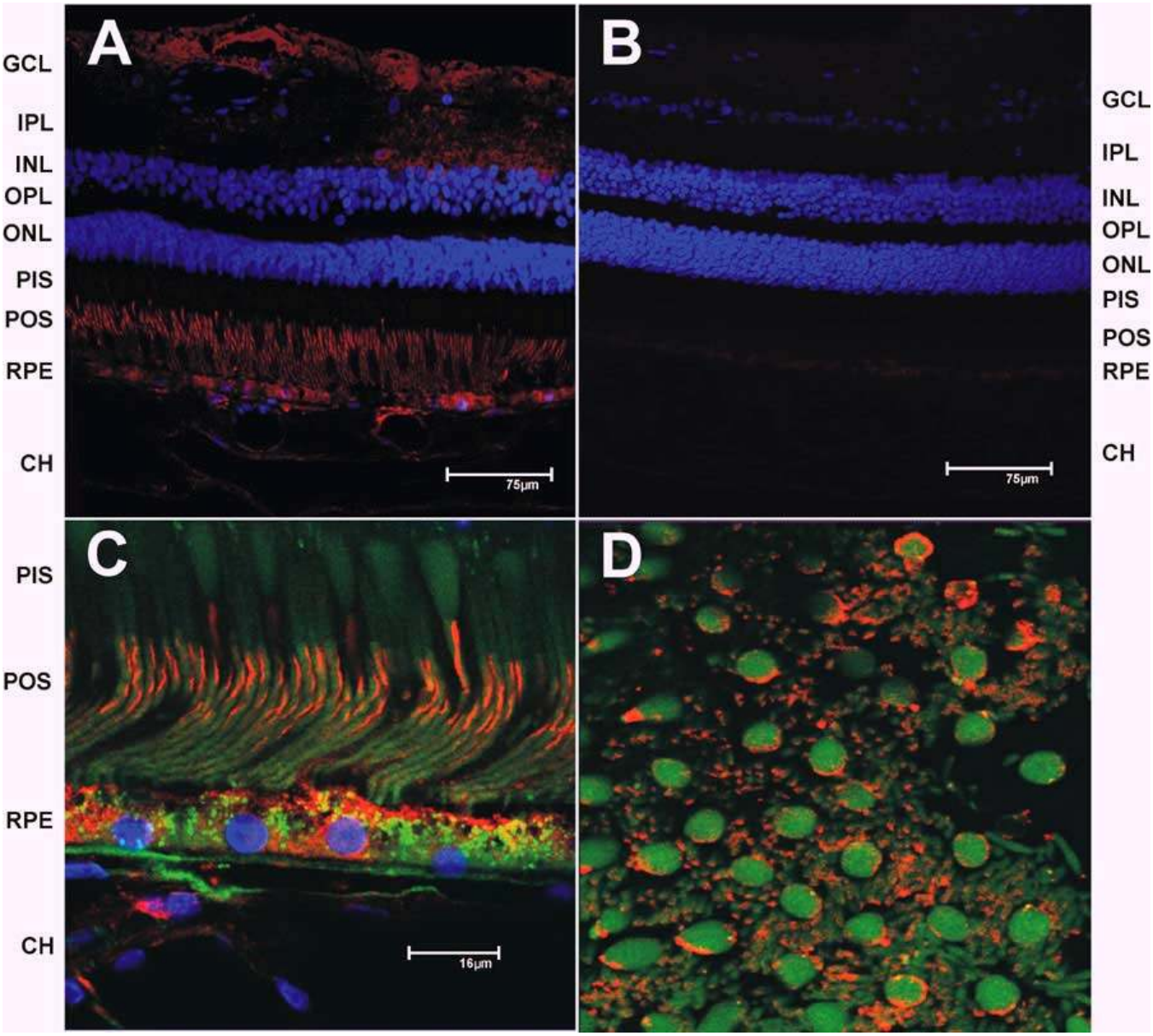

Figure 5. Immunohistochemical localization of SR-BII in monkey retina. The vibrotome sections from monkey retina were processed for immunhistochemistry and imaged by fluorescent confocal microscopy (see Materials and Methods). Nuclei were stained with DAPI (blue) and immunoreactivity was detected using a Cy5 conjugated secondary antibodies (red). **A**: SR-BII immunoreactivity detected with anti SR-BII peptide CLLEDSLSGQPTSAMA (cross-reacts with many species) rabbit polyclonal antibody (Abcam Inc.) at 1:50 dilution. **B**: No primary antibody control. **C**: SR-BII immunoreactivity at higher magnification focusing on the photoreceptors and retinal pigment epithelium/choriocapillaris regions. **D**: Cross section of photoreceptor region near connecting cilium region. Images **C** and **D** are shown with the green channel to take advantage of the retinal autofluorescence and provide better structural definition. Capillaries in **C** were stained with isolectin IB4 (green). Scale bars were included with each image.

ure 1) in the retina suggests that the retina has the capacity to engage in HDL particle maturation. Thus, we pursued correlative immunolocalization of LCAT and CETP in the retina in order to obtain additional information as to where this maturation process is most likely taking place in vivo.

LCAT synthesizes cholesterol esters in the blood to facilitate transport in lipoprotein particles [31]. In the monkey retina, LCAT immunoreactivity localized to the GCL, OPL, POS, RPE, and CH (Figure 7A). As was the case for apoA1 (see above), the soluble nature of LCAT suggests that its immunocytochemical localization within the POS layer likely indicates its presence in the IPM (Figure 7C). Immunolocalization of LCAT to the RPE further suggests that the RPE is a source of the IPM-associated LCAT. In addition, the presence of LCAT immunoreactivity in the GCL may be due, in part, to Müller cells; labeling in the OPL appears to be at or near the cone synaptic pedicles (Figure 7D, arrow). LCAT immunolabeling of the CH is expected for a protein abundant in serum.

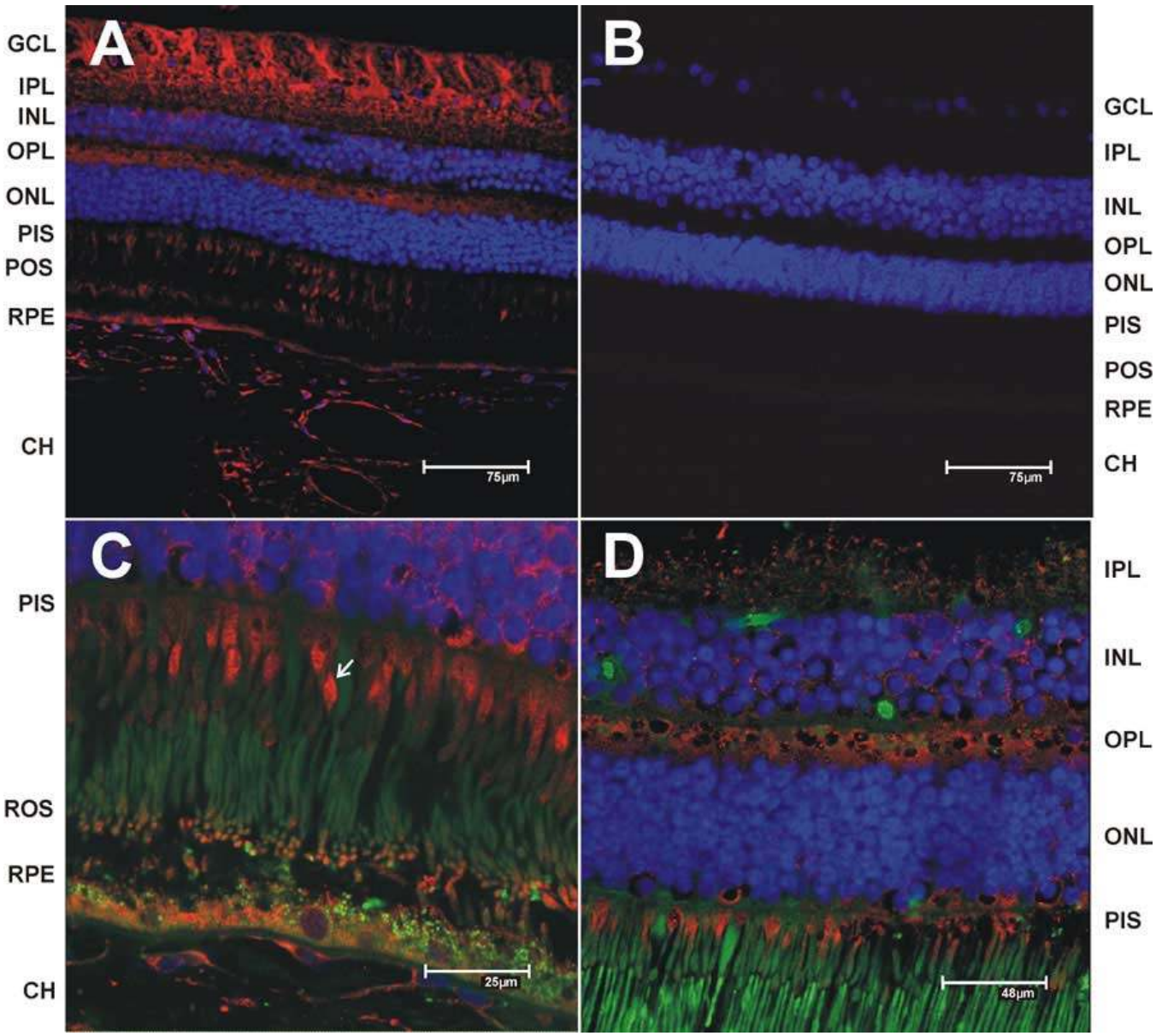

Figure 6. Immunohistochemical localization of CD36 in monkey retina. The vibrotome sections from monkey retina were processed for immunhistochemistry and imaged by fluorescent confocal microscopy (see Materials and Methods). Nuclei were stained with DAPI (blue) and immunoreactivity was detected using a Cy5 conjugated secondary antibodies (red). **A**: Immunoreactivity detected using an anti CD36 peptide AKENVTQDAEDNTVSF rabbit polyclonal antibody (Cayman Chemical, Ann Arbor, MI) at 1:50 dilution. **B**: No primary antibody control. **C**: CD36 immunoreactivity at higher magnification focusing on the photoreceptors and retinal pigment epithelium/choriocapillaris regions. **D**: CD36 immunoreactivity at higher magnification focusing on the OPL region. Images **C** and **D** are shown with the green channel to take advantage of the retinal autofluorescence and provide better structural definition. Capillaries in **D** were stained with isolectin IB4 (green). Scale bars were included with each image.

CETP transfers cholesterol esters from HDL to LDL particles [32]. In the monkey retina, CETP localized mainly to the POS and OPL (Figure 8). Like LCAT and apoA1, CETP is a secreted, soluble protein; thus, its presence in the POS layer likely reflects localization within the IPM (Figure 8C). CETP also localized to the OPL (Figure 8D), but in a more widespread pattern than that observed for LCAT; in addition, areas surrounding cone synaptic pedicles were also immunolabeled. Some labeling of the CH was also observed (Figure 8A,D), as expected for a serum-associated protein.

DISCUSSION

Although much is known about systemic lipid transport, relatively little is known about how lipids are taken up by the retina and how they are transported within the retina, both between and within retinal cells. In our companion paper [1],

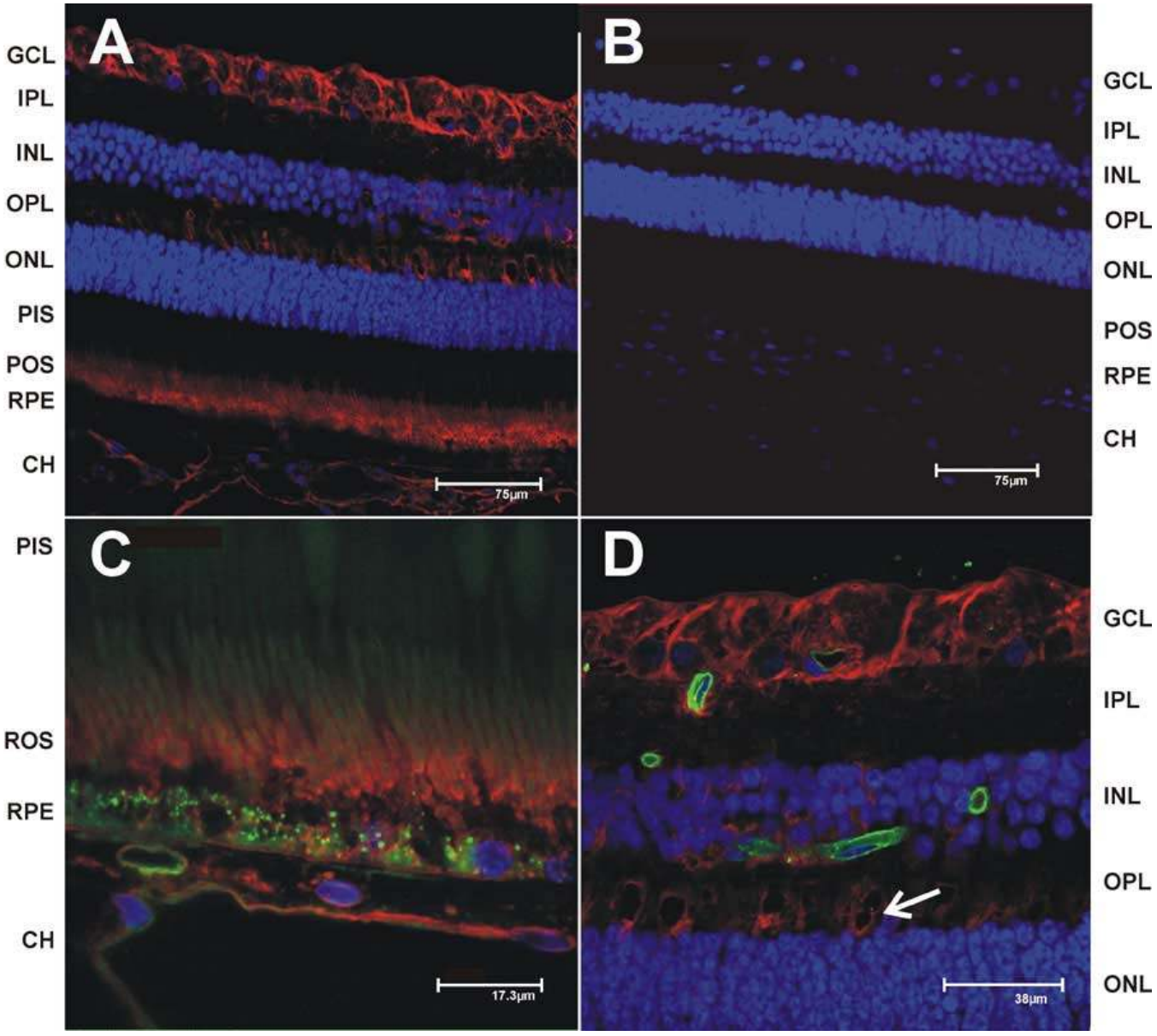

Figure 7. Immunohistochemical localization of lecithin:cholesterol acyltransferase in monkey retina. The vibrotome sections from monkey retina were processed for immunhistochemistry and imaged by fluorescent confocal microscopy (see Materials and Methods). Nuclei were stained with DAPI (blue) and immunoreactivity was detected using a Cy5 conjugated secondary antibodies (red). **A**: Lecithin:cholesterol acyltransferase (LCAT) was localized using a rabbit polyclonal to a recombinant C-terminus peptide (Abcam Inc. Cambridge, MA) at 1:1000. **B**: No primary antibody control. **C**: LCAT immunoreactivity at higher magnification focusing on the photoreceptors and retinal pigment epithelium/choriocapillaris regions. **D**: LCAT immunoreactivity at higher magnification focusing on the OPL and GCL regions. Primer pairs used for the RT-PCR analyses of the different genes shown in Fig. 1. The GenBank accession numbers for the cDNAs from which the primers were selected are shown in the right side column. The products generated were sequenced to confirm their authenticity. Images **C** and **D** are shown with the green channel to take advantage of the retinal autofluorescence and provide better structural definition. Capillaries in **D** were stained with isolectin IB4 (green). Scale bars were included with each image.

we demonstrated that the rat retina is able to take up circulating LDL and, to a lesser extent, HDL particles. Using a combination of a fluorescent cholesterol analog (cholestatrienol, CTL) and deuterated cholesterol incorporated into LDL and HDL particles, we were able to image and quantify the uptake of circulating LDL by the retina. This uptake process is apparently mediated by LDL receptors present mainly in RPE cells. However, these findings raised a series of questions concerning the subsequent transcytosis and intraretinal transport of these lipoprotein-derived lipids within the retina. In this subsequent study we have begun to address these questions by first identifying and localizing some of the main proteins known to mediate the systemic cholesterol efflux and transport pathways. Herein, we demonstrated, using monkey retina protein extracts (Figure 1A) and human RNA (Figure 1B), that the primate retina expresses most of the principle proteins involved in systemic lipid transport, including ABCA1, apoA1, apoE, SR-BI, SR-BII, CD36, LCAT, and CETP.

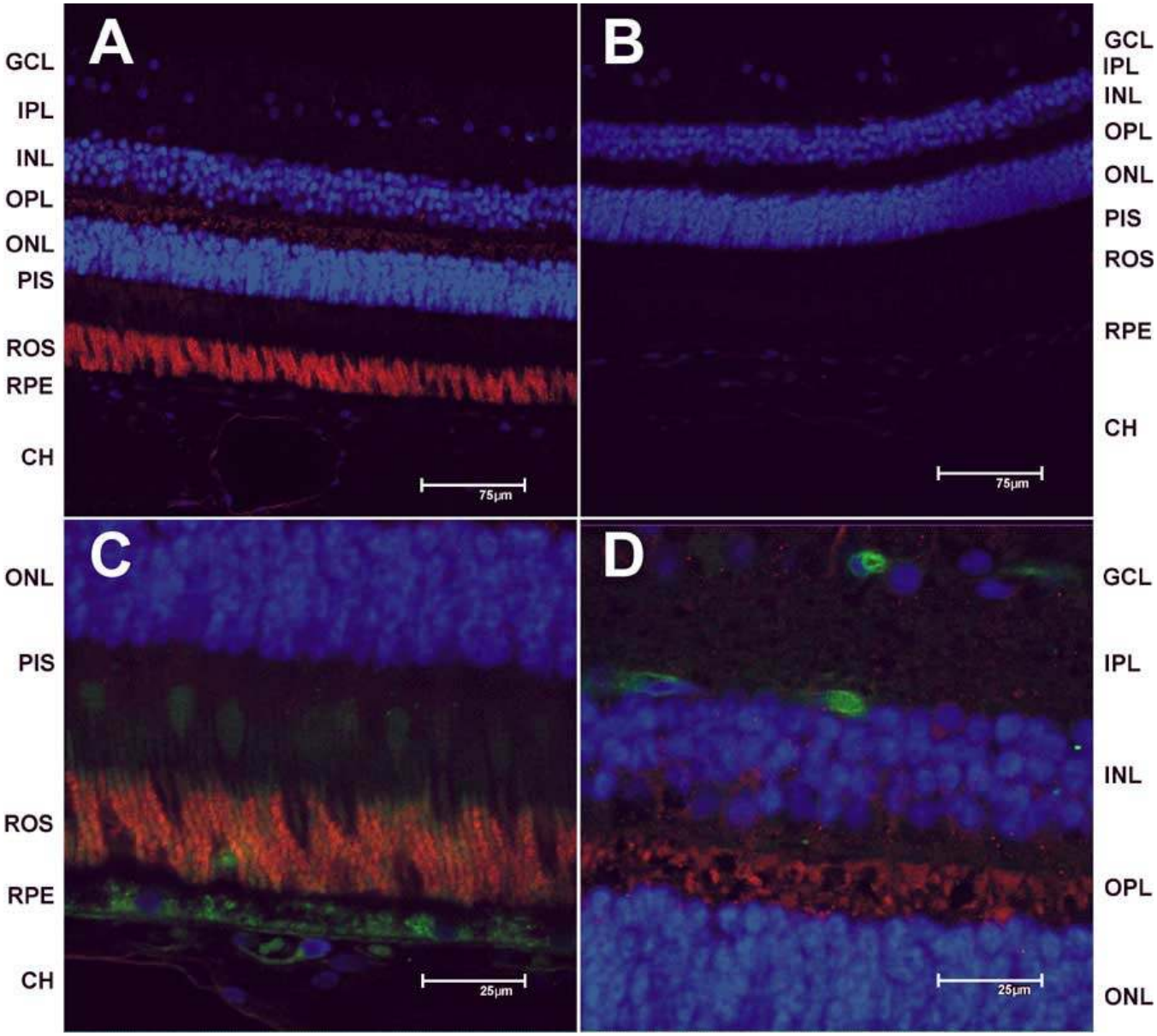

Figure 8. Immunohistochemical localization of cholesteryl ester transfer protein in monkey retina. The vibrotome sections from monkey retina were processed for immunhistochemistry and imaged by fluorescent confocal microscopy (see Materials and Methods). Nuclei were stained with DAPI (blue) and immunoreactivity was detected using a Cy5 conjugated secondary antibodies (red). **A**: cholesteryl ester transfer protein (CETP) was localized using anti-human CETP (synthetic C-terminus peptide) rabbit polyclonal antibody (BioVision Research Products, Mountain View, CA) at 1:50 dilution. **B**: No primary antibody control. **C**: CETP immunoreactivity at higher magnification focusing on the photoreceptors and retinal pigment epithelium/choriocapillaris regions. **D**: CETP immunoreactivity at higher magnification focusing on the outer plexiform layer region. Images **C** and **D** are shown with the green channel to take advantage of the retinal autofluorescence and provide better structural definition. Capillaries in **D** were stained with isolectin IB4 (green). Scale bars were included with each image.

ABCA1 is a well-characterized lipoprotein transporter known to be involved in the cholesterol efflux pathway in the liver [9-11,13]. In the monkey retina, ABCA1 localized to the GCL and OPL with some possible Müller cell involvement (Figure 2). The labeling of the OPL suggests possible lipoprotein trafficking in and/or around the synaptic terminals. The macula seems to be more strongly labeled than the peripheral retina. For the GCL and OPL this may be explained by the greater number of ganglion cells present in the macular region. However, the more intense labeling of the macular, compared to peripheral, RPE seems to reflect geographic differences in lipid transport activity that are determined by inherent differences in the resident RPE cells in these retinal regions (Figure 2C). Both the apical and basal aspects of the RPE exhibit ABCA1 immunolabeling (Figure 2C). This suggests that the RPE may be capable of transporting HDL both into and out of the retina. One conceivable role for such a process would be the elimination of cytotoxic oxidized lipids from the retina in the form of HDL-like lipid particles. Immunoblots detected the 220 kDa form of ABCA1 in the monkey RPE/choroid (Figure 1A, ABCA1 No. 2) and in two human-derived RPE cell lines (ABCA1 No. 3&4, ARPE19 and D407, respectively). However, in the neural retina (Figure 1A, ABCA1 No. 1), only a 65 kDa band was observed. This likely represents a proteolytically processed product and may be indicative of a higher turnover of ABCA1 in the neural retina. In addition, ABCA1 mRNA was readily detected in human neural retina (Figure 1B).

ApoA1, the dominant protein constituent of HDL particles, is the main lipoprotein transported by ABCA1 [13]. In the monkey retina, apoA1 was observed in the neural retina as well as in the RPE and choroid (Figure 3A). In the RPE, apoA1 localized mainly to the apical region, facing the IPM. We also observed apoA1 within Bruch's membrane (Figure 3C). However, since Bruch's membrane is bordered on one side by the fenestrated capillaries of the choriocapillaris and on the other side by the RPE, the origin of apoA1 (RPE versus blood) in Bruch's membrane cannot be determined by this technique. In the photoreceptor layer, apoA1 (like ABCA1) was observed in the rod inner segments (Figure 3C, arrow), but not in the cones. The reason(s) for this differential distribution among photoreceptor types is not clear at this time. There also was some immunoreactivity associated with the photoreceptor outer segments; considering the secreted nature of apoA1, this immunoreactivity most likely represents HDL or HDL-like particles resident in (secreted into and perhaps traveling through) the interphotoreceptor matrix. Immunoblot analysis (Figure 1A, apoA1) detected apoA1 as a ca. 62 kDa dimer in the monkey neural retina and RPE-choroid (lanes 1 and 2, respectively). ApoA1 is well-known to self-associate in the lipid-free state [12]. However, no apoA1 was detected in two different lines of cultured RPE cells, although it was detectable in the conditioned media from these cells (data not shown). ApoA1 mRNA was also readily detected in specimens of human neural retina (Figure 1B). These results are consistent with those reported by Li et al. [41], which demonstrated the immunolocalization of apoA1 to Bruch's membrane in postmortem human eye specimens as well as the presence of apoA1 transcripts (by RT-PCR) in RPE and neural retina. In that same report, the presence of atypical, heterogeneous lipoprotein-like particles isolated from human RPE-choroid were described; the density profile, lipid composition, and size were distinct from typical plasma lipoproteins, but the particles did contain apoA1 and apoB. The authors interpreted the results to mean that the

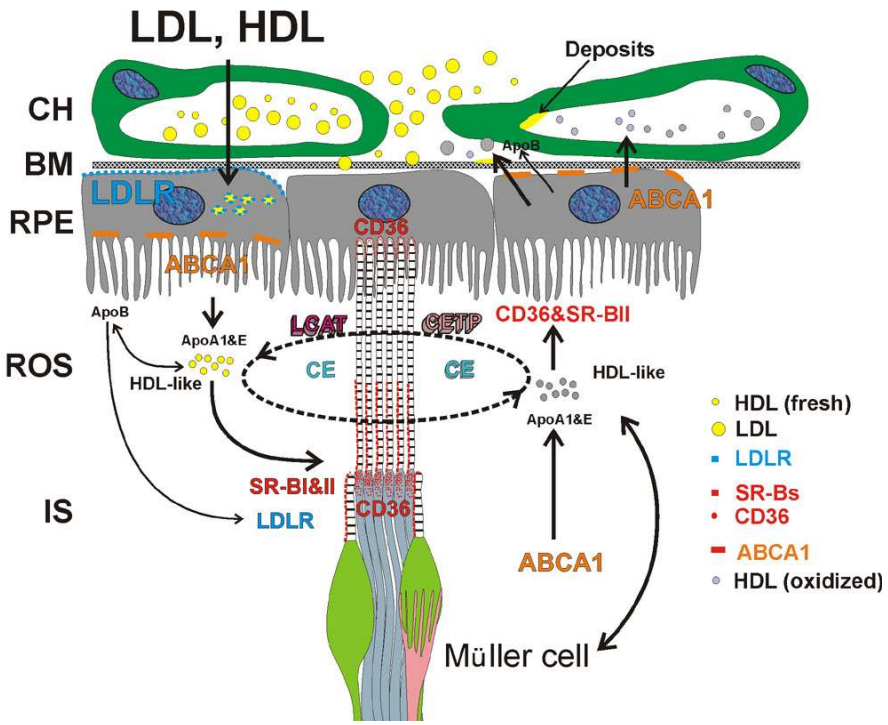

Figure 9. Proposed mechanism of lipid transport in the retina. Circulating high density lipoprotein (HDL) and low density lipoprotein (LDL) enter the retina via the SR-Bs and low density lipoprotein receptor (LDLR) in the retinal pigment epithelium (RPE). The RPE breaks-up the LDL and reassembles HDL-like particles using apoA1 and apoE, which are secreted into the interphotoreceptor matrix (IPM) via the ABCA1 transporter. The HDL particles take up additional lipids with the help of lecithin:cholesterol acyltransferase and cholesteryl ester transfer protein in the IPM. Lipids move back and forth between the RPE and the photoreceptors using HDL-like particles as intermediates and the SR-Bs and CD36 as receptors. The SR-Bs and CD36 may help to sort lipid particles with high oxidized lipid content. Müller cells may also play a role in delivering and accepting lipoprotein particles from the RPE and photoreceptors. The RPE may also secrete LDL and HDL-like particles back to the circulation to maintain homeostasis.

RPE and retina have the capacity to assemble and secrete lipoprotein-like particles, some of which end up being deposited as drusen components associated with Bruch's membrane. In sum, considering the known role of ABCA1 and apoA1 in HDL-dependent systemic lipid transport and the presence of ABCA1 and apoA1 in specific compartments of the retina, these data support the existence of an HDL-based intraretinal lipid transport mechanism.

The class B scavenger receptors, SR-BI and SR-BII, are nearly identical, differing only by a small peptide in the extreme C-terminus region that arises by alternative gene splicing [25,26,28]. The presence of the SR-BI and -BII receptors has been previously reported in RPE cells [34,35]. In the monkey retina, we found SR-BI localized to the choriocapillaris, ganglion cells and Müller cells, as well as the photoreceptors (Figure 4). In the photoreceptors, SR-BI was observed to localize to the cone and rod outer segments (Figure 4C). In the rod cells, the distribution of SR-BI was remarkably asymmetric, suggesting association with microtubules, whereas in the cones the distribution was more uniform and diffuse. This differential distribution in rods and cones suggests that SR-BI may serve different functions in these two distinct photoreceptor cell types. The reason for the apparent low expression of SR-BI in the RPE is unclear, since other investigators have demonstrated SR-BI present in primary RPE cells [35]. Immunoblots detected SR-BI in the monkey neural retina tissues and RPE-choroid (Figure 1A, SR-BI, lanes 1 and 2) as well as in the cultured RPE cells (Figure 1A, SR-BI, lanes 3 and 4). In neural retina, SR-BI was detected as multiple immunopositive bands, with the largest having an apparent molecular weight consistent with the fully glycosylated peptide (ca. 82 kDa). Another densely-stained band was found around ca 57 kDa, which is the predicted size of the unglycosylated peptide [24]. These receptors are glycoproteins, and contain 11 potential sites of N-glycosylation [24]; hence, differential glycosylation may explain, in part, the multiplicity of immunopositive bands observed. In addition, SR-BI receptors are also known to be associated with caveolin-1 in extra-hepatic tissues, where they tend to be relatively rapidly degraded [24]. We suspect that rapid turnover and degradation of these receptors in the retina may also underlie the multiple immunopositive bands observed.

SR-BII localized to RPE, ganglion and Müller cells, as well as to photoreceptor outer segments (Figure 5). The immunolabeling pattern was similar to that observed for SR-BI, but with two notable exceptions. First, SR-BII seems to localize to the base of the outer segments around the connecting cilium of both the cones and rods (Figure 5A), but its distribution does not extend as far up the outer segments as does that of SR-BI. This was confirmed by sectioning the photoreceptors horizontally, approximately at the section plane wherein the inner and outer segments meet (data not shown). The one-sided localization in the outer segments also suggests possible association with microtubules. In addition, SR-BII localized to both the apical and basal aspects of the RPE (Figure 5C). Immunoblots (Figure 1A, SR-BII) of monkey neural retina showed a series of SR-BII immunopositive bands, with the largest having an approximate molecular weight of ca. 51 kDa, which is similar to that of the predicted size of the unglycosylated peptide (ca. 56 kDa), but considerably smaller than that of the fully glycosylated isoform (ca. 82-85 kDa). In the RPE/CH fraction, only a around 20 kDa SR-BII-immunopositive band was detected by Western analysis (Figure 1A). The immunoblot suggests that most of the SR-BII is in the neural retina, with comparatively little in the RPE/CH. This is consistent with the immunohistochemical results (Figure 5), which demonstrated only faint immunoreactivity in the choriocapillaris. In cultured RPE cells SR-BII immunoreactivity was low in comparison with that observed in monkey retina (Figure 1, SR-BII). Thus, our results significantly extend the previously published observations concerning the distribution of these two scavenger receptors [34,35] by demonstrating the presence and distribution of SR-BI and -BII across the entire primate retina, especially the unusual, asymmetrical distribution in photoreceptor outer segments, which has not been reported heretofore.

The CD36 receptor is known to be involved (along with $\alpha v\beta 5$ integrin) in photoreceptor outer segment phagocytosis [37-40]. CD36 has been previously localized to the RPE [39,40], but its expression in other areas of the retina had not been previously reported. Herein, we demonstrated that CD36 is localized throughout the monkey retina (Figure 6). In the neural retina CD36 was observed in the ganglion and Müller cells (Figure 6A); the outer plexiform layer was also labeled (Figure 6D), suggesting localization to the photoreceptor synapses and/or horizontal cells. The rod photoreceptor inner segments were strongly labeled, but cone inner segments were not (Figure 6C). The RPE demonstrated a punctuate-like labeling distinct from the lipofuscin granules. In addition, the tips of the outer segments were brightly labeled (Figure 6C) consistent with the known role of this receptor in the phagocytosis of rod outer segments by the RPE [37-40]. The outer segment tip labeling is also reminiscent of that observed in a prior study employing cultured RPE cells fed isolated rod outer segments [42]. Immunoblots also confirm the presence of CD36 in the monkey retina (Figure 1A) and RT-PCR demonstrated its presence in human neural retina mRNA.

The CD36 receptor has been well studied in macrophages, where it serves to recognize oxidized LDL particles [30]. Recently, CD36 has been found to specifically recognize phosphocholine headgroups of oxidized phospholipids present on the surface of the oxidized lipid particles [29]. The finding of CD36 in the neural retina raises a number of questions concerning other roles of this receptor in the internalization and metabolism of oxidized lipid particles beyond those derived from photoreceptor outer segments. The SR-BI receptor is also known to bind oxidized LDL particles [42], suggesting a possible complementary role to CD36. Notably, our findings concerning CD36 expression and distribution in the neural retina differ from those previously reported [37], which demonstrated a complete absence of CD36 in the neural retina of rats (although it clearly was present in RPE cells). Although the reasons for this apparent discrepancy are unclear at this time, it could simply reflect a species-specific difference.

The expression of LCAT and CETP in the monkey retina has some very interesting implications (Figure 1), since it suggest the potential of cholesteryl ester (CE) synthesis and transfer to HDL-like particles [33]. LCAT uses lethicin and cholesterol to form lysolecithin and cholesteryl esters, which are then incorporated into immature HDL particles [21,23,31]. In humans, LCAT deficiency results in lower levels of CE in HDL and faster apoA1 degradation with no increased risk of atherosclerosis [43,44]. The immunoblot detected the expected size band for LCAT (ca. 62-65 kDa) in the monkey retina and RPE (Figure 1, LCAT lanes 1 and 2, respectively). RT-PCR also confirmed the presence of LCAT mRNA in human retina. LCAT immunoreactivity was localized in the monkey retina to the ganglion cells, Müller cells and photoreceptor outer segments (Figure 7A). The soluble and secreted nature of LCAT and its localization surrounding the outer tips of the photoreceptors suggest the activity in the IPM (Figure 7C). Immunolocalization in the OPL seems to mostly surround the cone synaptic pedicles (Figure 7D). The ganglion cells seem to also be capable of secreting LCAT (Figure 7D). The results suggest that the ganglion cells, photoreceptors and RPE may be synthesizing and secreting LCAT and thus these locations are areas of active CE synthesis.

In the systemic circulation, CETP promotes the transfer of CE from HDL to apoB (LDL and VLDL). In humans, CETP deficiency is associated with higher HDL and lower LDL levels in plasma and a reduced risk of cardiovascular disease [32]. CETP deficiency is also associated with a slower apoA1 catabolism and higher CE accumulation in HDL [45]. Herein, we showed that CETP localized to the outer plexiform layer and the photoreceptor outer segments (Figure 8A) in monkey retina. Since CETP, like LCAT, is a soluble, secreted protein, its association with the photoreceptor outer segments suggests activity in the inter-photoreceptor matrix (Figure 8C). Like LCAT, CETP is also localized to the OPL, but unlike LCAT, CETP was not readily detected in the ganglion cell layer (Figure 8D). The apparent low levels of apoB in the retina suggest that CETP may have a different function in the retina than in serum. CETP may be aiding in the transfer of CE from membranes or other lipoproteins not necessarily involving LDL particles. Thus, the presence of LCAT and CETP in the sames areas of the retina suggests that the retina has the ability to mature HDL particles and to transfer CE between lipoproteins. The association of both of these proteins with the rod and cone outer segments indicates this process may be critical to photoreceptor function (e.g., outer segment lipid turnover and renewal).

ApoE is a known lipid transporter in neural tissue [46] that has been shown to interact with SR-BI while in lipid-free form, but not when associated with lipids [15]. This apoE-SR-BI interaction seems to enhance the selective uptake of the SR-BI receptor for cholesterol esters from HDL [15]. The intracellular transport and secretion of apoE, like that of apoA1, is controlled by ABCA1 [14]. ApoE is known to be expressed in the retina [16-20], being present primarily in Müller cells and astrocytes, but also is found in the photoreceptor outer segment layer, ganglion cells, RPE and Bruch's membrane. These findings support the proposed role of apoE as a lipid transporter in the retina [16-18,20]. For the sake of completeness and to correlate apoE with the other lipid transport molecules, we included apoE in the immunoblot and RT-PCR analyses (Figure 1A and B). ApoE was detected as the expected 38 kDa peptide in monkey retinal tissues (Figure 1A lanes 1 and 2), but not in the RPE-derived cell lines (Figure 1A, lanes 3 and 4).

Based upon the findings obtained from our experiments employing cholestratrienol-labeled LDL and HDL [1] as well as the results of the present study demonstrating the presence and location of several well-characterized lipid transport proteins, we now propose a novel schematic to describe lipid transport in the retina (Figure 9). We hypothesize that this pathway is used by the retina particularly to facilitate the uptake and turnover of normal (non-oxidized) lipid species in retinal cells, but also may facilitate removal of oxidized lipids, especially those arising in the membranes of the photoreceptor outer segments. Per this scheme, the RPE and possibly the Müller cells take up lipoprotein particles and transfer the lipids into their endogenous apoA1- and apoE-containing HDL-like particles. These HDL-like particles are then transported by the ABCA1 (Figure 2) out of the RPE to deliver lipids to the SR-BI and -BII receptors associated with the photoreceptor outer segments (Figure 4, Figure 5). The presence of ABCA1 and apoA1 in the rod inner segments (Figure 2, Figure 3) suggests that the rods may be able to form and transport apoA1-containing HDL-like particles. The presence of apoB in the apical RPE and outer segments [1], coupled with the presence of LCAT and CETP in the outer segments (Figure 7, Figure 8), suggests that LDL (or LDL-like particles) may be also used as platforms for CE synthesis and transfer. Thus, photoreceptor cells (including their outer segments) possess the necessary components for HDL particle maturation. It should be noted that the interplay between glia and neurons in shuttling lipoprotein-bound lipids within nervous tissue has been conceptually advanced by Pfrieger and coworkers [47,48], who have proposed a critical role of glia-derived cholesterol in neuronal synaptogenesis in the central nervous system. Our current model more broadly considers extraretinal as well as intraretinal sources and transport mechanisms that underlie lipid homeostasis in the retina, particularly as it relates to cholesterol homeostasis.

There are multiple likely reasons for the elaboration of an extensive lipid transport mechanism in the retina, especially one involving the RPE and photoreceptor cells. Paramount is the need to support the assembly of photoreceptor outer segments, a vigorous, energetically demanding, substrate-intensive process that occurs continuously on a daily basis throughout the lifetime of those cells [49]. However, there may be other reasons for the extensive lipid uptake and transport. Lipids are a good source of energy and are involved in a variety of cellular processes. The retina is also the only neural tissue that has direct and frequent exposure to light. This presents a significant problem, because many lipids, especially polyunsaturated fatty acids and cholesterol esters, are highly susceptible to photo-oxidation [50], and the retina (particu-

larly the photoreceptor outer segments) is highly enriched in polyunsaturated fatty acids [51]. Although we are not presenting any evidence for lipid oxidation in this study, the presence of the receptor CD36, with its strict recognition of phosphatidylcholine-based oxidized phospholipids [29] in the RPE, the rod inner segments, photoreceptor synapses and ganglion cells (Figure 6), suggests a need to transport oxidized lipoprotein particles. The presence of ABCA1 and apoA1 also in those locations suggests the capacity for those cells to export of HDL-like particles. Oxidized lipids, particularly oxysterols, are often extremely toxic to cells, inducing apoptosis, gene expression changes, and immune responses in a number of different cells and tissues [52-56]. A recent study has also demonstrated that the retina expresses relatively high levels of the enzyme CYP27A1 (sterol 27-hydroxylase), which is capable of hydroxylating and neutralizing 7-ketocholsterol, a highly cytotoxic oxysterol [57]. Thus, this lipid transport mechanism may also serve to supply new, unoxidized lipids to the photoreceptor cells, as well a means by which deleterious oxidized lipids can be removed from the photoreceptors and other cells within the neural retina, repackaging and excreting them via the RPE and Müller cells to the circulation.

ACKNOWLEDGEMENTS

The authors would like to thank Dr. Robert Fariss, Dr. Mercedes Campos and Mr. Kent Sheridan for his help with the immunohistochemistry of the CD36 and SR-BII receptors. We would like to thank Dr. Richard C. Hunt for his kind gift of D407 cells. This work was supported by the National Eye Institute intramural research program. SJF was supported, in part, by U.S.P.H.S. grant EY007361, by the Norman J. Stupp Foundation Charitable Trust, and by an unrestricted grant from Research to Prevent Blindness.

REFERENCES

1. Tserentsoodol N, Sztein J, Campos M, Gordiyenko NV, Fariss RN, Lee JW, Fliesler SJ, Rodriguez IR. Mol Vis 2006; 12:1306-18.
2. Fischer RT, Stephenson FA, Shafiee A, Schroeder F. delta 5,7,9(11)-Cholestatrien-3 beta-ol: a fluorescent cholesterol analogue. Chem Phys Lipids 1984; 36:1-14.
3. Sacks FM, Pfeffer MA, Moye LA, Rouleau JL, Rutherford JD, Cole TG, Brown L, Warnica JW, Arnold JM, Wun CC, Davis BR, Braunwald E. The effect of pravastatin on coronary events after myocardial infarction in patients with average cholesterol levels. Cholesterol and Recurrent Events Trial investigators. N Engl J Med 1996; 335:1001-9.
4. Noske UM, Schmidt-Erfurth U, Meyer C, Diddens H. [Lipid metabolism in retinal pigment epithelium. Possible significance of lipoprotein receptors]. Ophthalmologe 1998; 95:814-9.
5. Gordiyenko N, Campos M, Lee JW, Fariss RN, Sztein J, Rodriguez IR. RPE cells internalize low-density lipoprotein (LDL) and oxidized LDL (oxLDL) in large quantities in vitro and in vivo. Invest Ophthalmol Vis Sci 2004; 45:2822-9.
6. Brown MS, Kovanen PT, Goldstein JL. Regulation of plasma cholesterol by lipoprotein receptors. Science 1981; 212:628-35.
7. Dietschy JM, Turley SD. Thematic review series: brain Lipids. Cholesterol metabolism in the central nervous system during early development and in the mature animal. J Lipid Res 2004; 45:1375-97.
8. Jeon H, Blacklow SC. Structure and physiologic function of the low-density lipoprotein receptor. Annu Rev Biochem 2005; 74:535-62.
9. Efferth T. Adenosine triphosphate-binding cassette transporter genes in ageing and age-related diseases. Ageing Res Rev 2003; 2:11-24.
10. Pohl A, Devaux PF, Herrmann A. Function of prokaryotic and eukaryotic ABC proteins in lipid transport. Biochim Biophys Acta 2005; 1733:29-52.
11. Yokoyama S. Assembly of high density lipoprotein by the ABCA1/apolipoprotein pathway. Curr Opin Lipidol 2005; 16:269-79.
12. Frank PG, Marcel YL. Apolipoprotein A-I: structure-function relationships. J Lipid Res 2000; 41:853-72.
13. Fitzgerald ML, Okuhira K, Short GF 3rd, Manning JJ, Bell SA, Freeman MW. ATP-binding cassette transporter A1 contains a novel C-terminal VFVNFA motif that is required for its cholesterol efflux and ApoA-I binding activities. J Biol Chem 2004; 279:48477-85.
14. Von Eckardstein A, Langer C, Engel T, Schaukal I, Cignarella A, Reinhardt J, Lorkowski S, Li Z, Zhou X, Cullen P, Assmann G. ATP binding cassette transporter ABCA1 modulates the secretion of apolipoprotein E from human monocyte-derived macrophages. FASEB J 2001; 15:1555-61.
15. Bultel-Brienne S, Lestavel S, Pilon A, Laffont I, Tailleux A, Fruchart JC, Siest G, Clavey V. Lipid free apolipoprotein E binds to the class B Type I scavenger receptor I (SR-BI) and enhances cholesteryl ester uptake from lipoproteins. J Biol Chem 2002; 277:36092-9.
16. Amaratunga A, Abraham CR, Edwards RB, Sandell JH, Schreiber BM, Fine RE. Apolipoprotein E is synthesized in the retina by Muller glial cells, secreted into the vitreous, and rapidly transported into the optic nerve by retinal ganglion cells. J Biol Chem 1996; 271:5628-32.
17. Kuhrt H, Hartig W, Grimm D, Faude F, Kasper M, Reichenbach A. Changes in CD44 and ApoE immunoreactivities due to retinal pathology of man and rat. J Hirnforsch 1997; 38:223-9.
18. Shanmugaratnam J, Berg E, Kimerer L, Johnson RJ, Amaratunga A, Schreiber BM, Fine RE. Retinal Muller glia secrete apolipoproteins E and J which are efficiently assembled into lipoprotein particles. Brain Res Mol Brain Res 1997; 50:113-20.
19. Anderson DH, Ozaki S, Nealon M, Neitz J, Mullins RF, Hageman GS, Johnson LV. Local cellular sources of apolipoprotein E in the human retina and retinal pigmented epithelium: implications for the process of drusen formation. Am J Ophthalmol 2001; 131:767-81.
20. Ishida BY, Bailey KR, Duncan KG, Chalkley RJ, Burlingame AL, Kane JP, Schwartz DM. Regulated expression of apolipoprotein E by human retinal pigment epithelial cells. J Lipid Res 2004; 45:263-71.
21. Small DM. Mechanisms of reversed cholesterol transport. Agents Actions Suppl 1988; 26:135-46.
22. Skinner ER. High-density lipoprotein subclasses. Curr Opin Lipidol 1994; 5:241-7.
23. Wang M, Briggs MR. HDL: the metabolism, function, and therapeutic importance. Chem Rev 2004; 104:119-37.
24. Rhainds D, Brissette L. The role of scavenger receptor class B type I (SR-BI) in lipid trafficking. defining the rules for lipid traders. Int J Biochem Cell Biol 2004; 36:39-77.
25. Webb NR, de Villiers WJ, Connell PM, de Beer FC, van der Westhuyzen DR. Alternative forms of the scavenger receptor BI (SR-BI). J Lipid Res 1997; 38:1490-5.

26. Webb NR, Connell PM, Graf GA, Smart EJ, de Villiers WJ, de Beer FC, van der Westhuyzen DR. SR-BII, an isoform of the scavenger receptor BI containing an alternate cytoplasmic tail, mediates lipid transfer between high density lipoprotein and cells. J Biol Chem 1998; 273:15241-8.
27. Eckhardt ER, Cai L, Sun B, Webb NR, van der Westhuyzen DR. High density lipoprotein uptake by scavenger receptor SR-BII. J Biol Chem 2004; 279:14372-81.
28. Webb NR, Cai L, Ziemba KS, Yu J, Kindy MS, van der Westhuyzen DR, de Beer FC. The fate of HDL particles in vivo after SR-BI-mediated selective lipid uptake. J Lipid Res 2002; 43:1890-8.
29. Boullier A, Friedman P, Harkewicz R, Hartvigsen K, Green SR, Almazan F, Dennis EA, Steinberg D, Witztum JL, Quehenberger O. Phosphocholine as a pattern recognition ligand for CD36. J Lipid Res 2005; 46:969-76.
30. Boullier A, Bird DA, Chang MK, Dennis EA, Friedman P, Gillotre-Taylor K, Horkko S, Palinski W, Quehenberger O, Shaw P, Steinberg D, Terpstra V, Witztum JL. Scavenger receptors, oxidized LDL, and atherosclerosis. Ann N Y Acad Sci 2001; 947:214-22;discussion222-3.
31. Ng DS. Insight into the role of LCAT from mouse models. Rev Endocr Metab Disord 2004; 5:311-8.
32. de Grooth GJ, Klerkx AH, Stroes ES, Stalenhoef AF, Kastelein JJ, Kuivenhoven JA. A review of CETP and its relation to atherosclerosis. J Lipid Res 2004; 45:1967-74.
33. Ohashi R, Mu H, Wang X, Yao Q, Chen C. Reverse cholesterol transport and cholesterol efflux in atherosclerosis. QJM 2005; 98:845-56.
34. Hayes KC, Lindsey S, Stephan ZF, Brecker D. Retinal pigment epithelium possesses both LDL and scavenger receptor activity. Invest Ophthalmol Vis Sci 1989; 30:225-32.
35. Duncan KG, Bailey KR, Kane JP, Schwartz DM. Human retinal pigment epithelial cells express scavenger receptors BI and BII. Biochem Biophys Res Commun 2002; 292:1017-22.
36. Connelly MA, Klein SM, Azhar S, Abumrad NA, Williams DL. Comparison of class B scavenger receptors, CD36 and scavenger receptor BI (SR-BI), shows that both receptors mediate high density lipoprotein-cholesteryl ester selective uptake but SR-BI exhibits a unique enhancement of cholesteryl ester uptake. J Biol Chem 1999; 274:41-7.
37. Ryeom SW, Sparrow JR, Silverstein RL. CD36 participates in the phagocytosis of rod outer segments by retinal pigment epithelium. J Cell Sci 1996; 109:387-95.
38. Ryeom SW, Silverstein RL, Scotto A, Sparrow JR. Binding of anionic phospholipids to retinal pigment epithelium may be mediated by the scavenger receptor CD36. J Biol Chem 1996; 271:20536-9.
39. Sparrow JR, Ryeom SW, Abumrad NA, Ibrahimi A, Silverstein RL. CD36 expression is altered in retinal pigment epithelial cells of the RCS rat. Exp Eye Res 1997; 64:45-56.
40. Finnemann SC, Silverstein RL. Differential roles of CD36 and alphavbeta5 integrin in photoreceptor phagocytosis by the retinal pigment epithelium. J Exp Med 2001; 194:1289-98.
41. Li CM, Chung BH, Presley JB, Malek G, Zhang X, Dashti N, Li L, Chen J, Bradley K, Kruth HS, Curcio CA. Lipoprotein-like particles and cholesteryl esters in human Bruch's membrane: initial characterization. Invest Ophthalmol Vis Sci 2005; 46:2576-86.
42. Gillotte-Taylor K, Boullier A, Witztum JL, Steinberg D, Quehenberger O. Scavenger receptor class B type I as a receptor for oxidized low density lipoprotein. J Lipid Res 2001; 42:1474-82.
43. Rader DJ, Ikewaki K, Duverger N, Schmidt H, Pritchard H, Frohlich J, Clerc M, Dumon MF, Fairwell T, Zech L, Nakamura H, Nagano M, and Brewer HB. Markedly accelerated catabolism of apolipoprotein A-II (ApoA-II) and high density lipoproteins containing ApoA-II in classic lecithin: cholesterol acyltransferase deficiency and fish-eye disease. J Clin Invest 1994; 93:321-30.
44. Ayyobi AF, McGladdery SH, Chan S, John Mancini GB, Hill JS, Frohlich JJ. Lecithin: cholesterol acyltransferase (LCAT) deficiency and risk of vascular disease: 25 year follow-up. Atherosclerosis 2004; 177:361-6.
45. Ikewaki K, Rader DJ, Sakamoto T, Nishiwaki M, Wakimoto N, Schaefer JR, Ishikawa T, Fairwell T, Zech LA, Nakamura H, Brewer HB. Delayed catabolism of high density lipoprotein apolipoproteins A-I and A-II in human cholesteryl ester transfer protein deficiency. J Clin Invest 1993; 92:1650-8.
46. Vance JE, Hayashi H, Karten B. Cholesterol homeostasis in neurons and glial cells. Semin Cell Dev Biol 2005; 16:193-212.
47. Goritz C, Mauch DH, Nagler K, Pfrieger FW. Role of glia-derived cholesterol in synaptogenesis: new revelations in the synapse-glia affair. J Physiol Paris 2002; 96:257-63.
48. Pfrieger FW. Cholesterol homeostasis and function in neurons of the central nervous system. Cell Mol Life Sci 2003; 60:1158-71.
49. Nguyen-Legros J, Hicks D. Renewal of photoreceptor outer segments and their phagocytosis by the retinal pigment epithelium. Int Rev Cytol 2000; 196:245-313.
50. Girotti AW, Kriska T. Role of lipid hydroperoxides in photo-oxidative stress signaling. Antioxid Redox Signal 2004; 6:301-10.
51. Fliesler SJ, Anderson RE. Chemistry and metabolism of lipids in the vertebrate retina. Prog Lipid Res 1983; 22:79-131.
52. Schroepfer GJ Jr. Oxysterols: modulators of cholesterol metabolism and other processes. Physiol Rev 2000; 80:361-554.
53. Panini SR, Sinensky MS. Mechanisms of oxysterol-induced apoptosis. Curr Opin Lipidol 2001; 12:529-33.
54. Colles SM, Maxson JM, Carlson SG, Chisolm GM. Oxidized LDL-induced injury and apoptosis in atherosclerosis. Potential roles for oxysterols. Trends Cardiovasc Med 2001; 11:131-8.
55. Salvayre R, Auge N, Benoist H, Negre-Salvayre A. Oxidized low-density lipoprotein-induced apoptosis. Biochim Biophys Acta 2002; 1585:213-21.
56. Leitinger N. Oxidized phospholipids as modulators of inflammation in atherosclerosis. Curr Opin Lipidol 2003; 14:421-30.
57. Lee JW, Fuda H, Javitt NB, Strott CA, Rodriguez IR. Expression and localization of sterol 27-hydroxylase (CYP27A1) in monkey retina. Exp Eye Res 2006; 83:465-9.

The print version of this article was created on 27 Oct 2006. This reflects all typographical corrections and errata to the article through that date. Details of any changes may be found in the online version of the article. α